PLOS GENETICS

RESEARCH ARTICLE

The Rab GTPase activating protein TBC-2 regulates endosomal localization of DAF-16 FOXO and lifespan

İçten Meraş[1,2,3], Laëtitia Chotard[2,4], Thomas Liontis[3,5,6], Zakaria Ratemi[3], Benjamin Wiles[3], Jung Hwa Seo[3], Jeremy M. Van Raamsdonk[3,4,5,6], Christian E. Rocheleau[1,2,3,4]*

1 Department of Anatomy and Cell Biology, McGill University, Montreal, Canada, **2** Division of Endocrinology and Metabolism, Department of Medicine, McGill University, Montreal, Canada, **3** Metabolic Disorders and Complications Program, Centre for Translational Biology, Research Institute of the McGill University Health Centre, Montreal, Canada, **4** Division of Experimental Medicine, Department of Medicine, McGill University, Montreal, Canada, **5** Department of Neurology and Neurosurgery, McGill University, Montreal, Canada, **6** Brain Repair and Integrative Neuroscience Program, Centre for Translational Biology, Research Institute of the McGill University Health Centre, Montreal, Canada

* christian.rocheleau@mcgill.ca

Citation: Meraş İ, Chotard L, Liontis T, Ratemi Z, Wiles B, Seo JH, et al. (2022) The Rab GTPase activating protein TBC-2 regulates endosomal localization of DAF-16 FOXO and lifespan. PLoS Genet 18(8): e1010328. https://doi.org/10.1371/journal.pgen.1010328

Editor: Gregory S. Barsh, HudsonAlpha Institute for Biotechnology, UNITED STATES

Received: May 20, 2022

Accepted: July 6, 2022

Published: August 1, 2022

Data Availability Statement: All relevant data are within the manuscript and its Supporting Information files.

Funding: This work was funded by Canadian Institutes of Health Research (https://cihr-irsc.gc.ca/) project grants PJT-159725 (to CER), PJT-399148 (to JMVR) and PJT-416150 (to JMVR). This work was also supported by the National Institute of General Medical Sciences (https://www.nigms.nih.gov/) R01: GM121756 (to JMVR) and a Natural Sciences and Engineering

Abstract

FOXO transcription factors have been shown to regulate longevity in model organisms and are associated with longevity in humans. To gain insight into how FOXO functions to increase lifespan, we examined the subcellular localization of DAF-16 in *C. elegans*. We show that DAF-16 is localized to endosomes and that this endosomal localization is increased by the insulin-IGF signaling (IIS) pathway. Endosomal localization of DAF-16 is modulated by endosomal trafficking proteins. Disruption of the Rab GTPase activating protein TBC-2 increases endosomal localization of DAF-16, while inhibition of TBC-2 targets, RAB-5 or RAB-7 GTPases, decreases endosomal localization of DAF-16. Importantly, the amount of DAF-16 that is localized to endosomes has functional consequences as increasing endosomal localization through mutations in *tbc-2* reduced the lifespan of long-lived *daf-2 IGFR* mutants, depleted their fat stores, and DAF-16 target gene expression. Overall, this work identifies endosomal localization as a mechanism regulating DAF-16 FOXO, which is important for its functions in metabolism and aging.

Author summary

FOXO transcription factors have been shown to modulate lifespan in multiple model organisms and to be associated with longevity in humans. Here we describe a new localization of the *C. elegans* FOXO transcription factor, called DAF-16. We report that DAF-16 localizes to endosomes, membrane compartments internalized from the plasma membrane at the cell surface. We demonstrate that expansion of these endosome compartments by disruption of an endosomal regulator called TBC-2 results in increased localization of DAF-16 on endosomes at the expense of nuclear localization in the

Research Council of Canada (https://www.nserc-crsng.gc.ca/) Discovery Grant RGPIN-2019-04302 (to JMVR). JMVR and TL received salary support from the Fonds de Recherche du Québec - Santé (https://frq.gouv.qc.ca/). The funders had no role in study design, data collection and analysis, decision to publish, or preparation of the manuscript.

Competing interests: The authors have declared that no competing interests exist.

intestinal cells. This results in altered expression of DAF-16 target genes, reduced fat storage and decreased lifespan. These results demonstrate the importance of endosomal trafficking for proper localization of DAF-16 and suggest that the endosome is an important site of FOXO regulation. An intriguing possibility based on our results is that storage of FOXO on endosomes facilitates the mobilization of FOXO as a rapid response to environmental stress.

Introduction

Insulin/insulin-like growth factor signaling (IIS) is an evolutionarily conserved pathway that plays an important role in lifespan, development, metabolism, immunity and stress responses from *Caenorhabditis elegans* to humans [1–4]. IIS-mediated regulation of *C. elegans* FOXO, DAF-16, was first identified via genetic characterization of mutants affecting dauer (an alternative stress resistant larval stage) and life span [5–8]. For example, animals that have a mutation in their insulin-like growth factor receptor (IGFR), DAF-2, live almost two times longer than wild-type animals in a DAF-16-dependent manner [6]. Under favorable conditions, the *C. elegans* DAF-2 IGFR signals through a conserved PI3K/Akt pathway to phosphorylate and inhibit nuclear accumulation of DAF-16 FOXO [1]. In short, DAF-2 IGFR activation leads to the activation of AGE-1 PI3K which phosphorylates $PI(4,5)P_2$ to generate $PI(3,4,5)P_3$, which can bind and recruit PDK-1 and AKT-1/2 kinases. DAF-18 PTEN, a lipid and protein phosphatase, countacts AGE-1 PI3K and thus negatively regulates signaling. PDK-1 activates AKT-1/2 which in turn phosphorylates DAF-16 creating binding sites for PAR-5 and FTT-2 14-3-3 scaffold proteins that sequester DAF-16 FOXO in the cytoplasm. During adverse conditions such as starvation, IIS is suppressed and DAF-16 FOXO enters the nucleus to induce the expression of stress response genes. As such, DAF-16 FOXO mediates most *daf-2 IGFR* mutant phenotypes.

Upon activation, the Insulin/IGF receptor is internalized into endosomes, where it can dissociate from its ligand and recycle back to the plasma membrane, or it can be targeted for lysosomal degradation [9]. The identification of activated IGFR on endosomes suggested that endosomes can serve as a platform for signaling [10]. Subsequently, several components of the IIS pathway have been shown to localize on endosomes. PTEN localizes on PI(3)P positive endosomes through its C2 domain and has been demonstrated to regulate endosome trafficking via dephosphorylation of Rab7 [11,12]. Akt2 localizes to Appl-1 and WDFY-2 positive endosomes to get fully activated and regulate Akt2 specific downstream substrates [13,14]. 14-3-3 proteins can interact with several Akt phosphorylation targets to regulate their subcellular localization and have been found on endosomes [15,16]. However, a role for endosome trafficking in regulation of FOXO transcription factors has not been demonstrated to the best of our knowledge.

Rab5 and Rab7 GTPases localize to early and late endosomes respectively and are critical regulators of trafficking to the lysosome, an organelle important for cargo degradation and metabolic signaling [17,18]. Like many small GTPases, Rabs cycle between a GTP-bound active state and GDP-bound inactive state. This cycling requires guanine nucleotide exchange factors for activation and GTPase Activating Proteins (GAPs) to catalyze GTP hydrolysis and hence Rab inactivation. We previously characterized *C. elegans* TBC-2 as having *in vitro* GAP activity towards RAB-5, and some activity towards RAB-7 [19]. Mutations in *tbc-2* result in enlarged late endosomes in several tissues including the intestine, an important site of IIS and metabolic regulation [20]. In addition to early to late endosome maturation, TBC-2 regulates

phagosome maturation [21], dense core vesicle maturation [22] endosome recycling as an effector of RAB-10 and CED-10/Rac [23,24] and yolk protein trafficking in oocytes and embryos [25]. Yolk protein is prematurely degraded in *tbc-2* mutants. As such, *tbc-2* mutant larvae hatched in the absence of food had reduced survival during L1 (first larval stage) diapause [25].

Here we explore the subcellular localization of DAF-16 and show that DAF-16 localizes on early and late endosomes in *C. elegans* intestinal cells. We found that endosome localization of DAF-16 is regulated by nutrient availability and IIS. We show that endosome localization of DAF-16 is increased through mutations in *tbc-2*, at the expense of nuclear localization. The increased endosomal localization of DAF-16 in *tbc-2* mutants decreases lifespan, fat storage and DAF-16 target gene expression in *daf-2 IGFR* mutant animals. These results demonstrate a role of endosomal localization in the regulation and function of DAF-16 FOXO.

Results

TBC-2 and the RAB-5 and RAB-7 GTPases regulate DAF-16 localization to endosomes in the intestine

We previously reported that *tbc-2* is required for survival during L1 diapause [25]. Since *daf-16* is also required for survival during L1 diapause [26,27] we sought to test whether TBC-2 might regulate the nuclear versus cytoplasmic localization of DAF-16. Although we determined that loss of *tbc-2* did not result in precocious development during L1 diapause as seen *daf-16* mutants [25,27], we found that TBC-2 does in fact regulate DAF-16 localization. Unexpectedly, we found that DAF-16a::GFP (*zIs356*) localized to numerous amorphous vesicles in the intestinal cells of *tbc-2(tm2241)* deletion mutant animals (Fig 1B). Furthermore, we found that DAF-16a::GFP localized to cytoplasmic vesicles in the intestine of wild-type animals (Fig 1A). The percentage of hermaphrodites with DAF-16 vesicles increased during larval development, peaking at L4 and young adults (Figs 1I and S1A). *tbc-2(tm2241)* animals were about twice as likely to have DAF-16 vesicles than wild type (Figs 1J and S1A). The number of DAF-16 positive vesicles in wild type can range from zero to hundreds (Fig 1I). DAF-16 positive vesicles can be distributed throughout all 20 intestinal cells or be present in high numbers in just a few cells. DAF-16a::GFP localization is not sex specific as we found similar numbers of DAF-16 positive vesicles in males as in hermaphrodites (S1B Fig). Although DAF-16a::GFP nuclear localization is low in normal growth conditions, we find that *tbc-2(tm2241)* intestinal nuclei appear to have less nuclear DAF-16a::GFP than wild type (Fig 1A and 1B). We quantified the fluorescence intensity of DAF-16a::GFP in nuclei of *tbc-2(tm2241)* intestinal cells comparing nuclei of cells with vesicles versus nuclei of cells without vesicles (Fig 1K). We found that nuclei of cells with DAF-16 positive vesicles have significantly less nuclear DAF-16a::GFP than cells without vesicles. Thus, DAF-16 localizes to vesicles in wild-type and *tbc-2(tm2241)* animals, and *tbc-2(tm2241)* animals have less nuclear DAF-16a::GFP, likely due to sequestration to cytoplasmic vesicles.

To determine if the localization of the GFP tag or the splice variant or expression levels affected DAF-16 vesicular localization we analyzed three other transgenic strains with lower expression levels; GFP::DAF-16a (*muIs71*), DAF-16a::RFP (*lpIs12*) and DAF-16f::GFP (*lpIs14*, with an alternative N-terminus)[28–30]. Using the three fluorescent reporters, we detected DAF-16 vesicles in the *tbc-2(tm2241)* mutant, albeit not in the wild-type background (S2G–S2X Fig). Overexpression of GFP from *vha-6* intestinal specific promoter, *vhEx1[Pvha-6::GFP]*, did not show significant vesicular localization in wild-type animals (S3A Fig). In *tbc-2(tm2241)* animals GFP showed some vesicular localization and potential aggregates, but much less than seen with DAF-16a::GFP, indicating that the vesicular localization is due to DAF-16

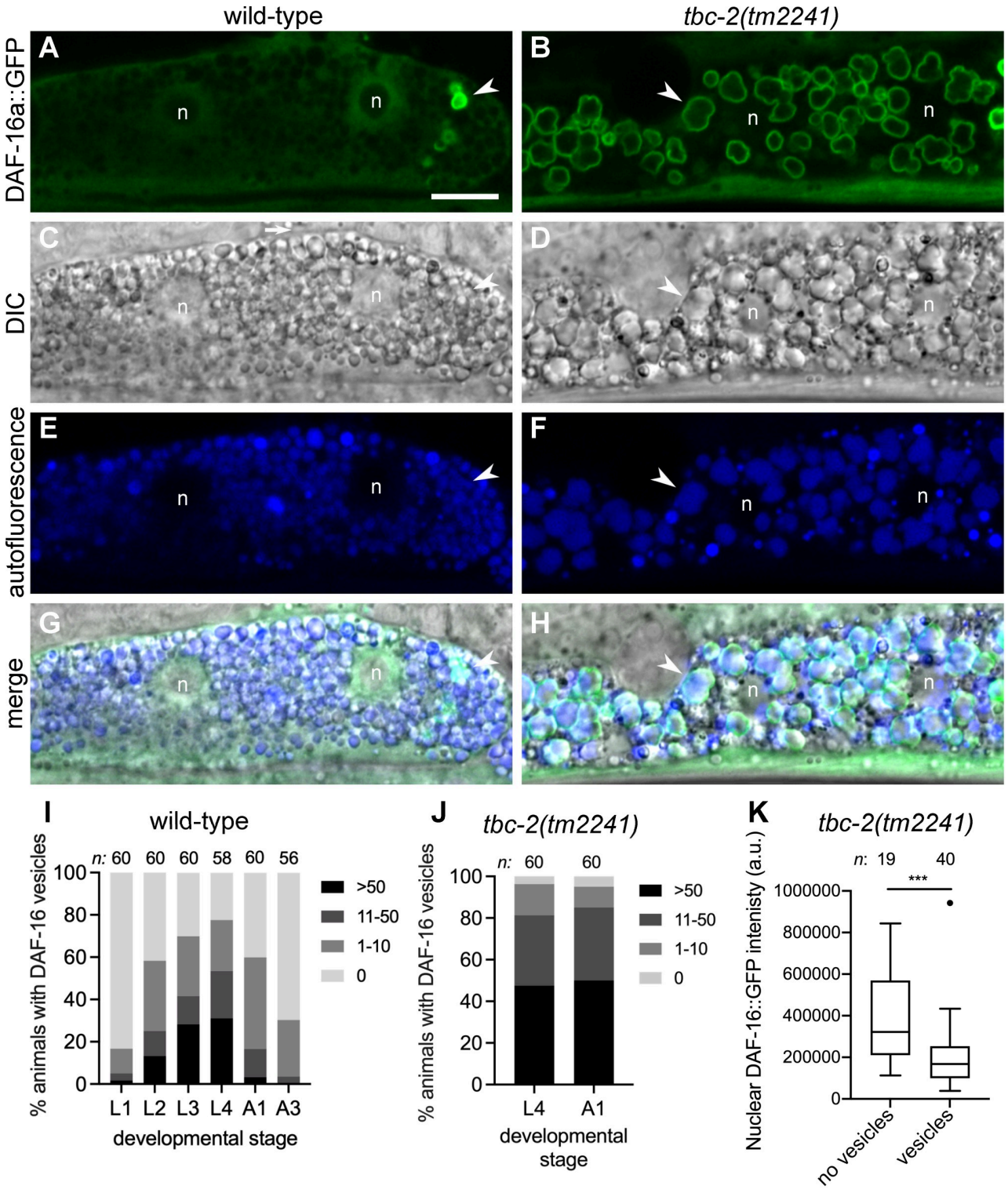

Fig 1. DAF-16 FOXO localizes to vesicles in intestinal cells. (A-H) Representative confocal and differential interference contrast (DIC) images of an intestinal cell of wild-type (A, C, E, G) and *tbc-2(tm2241)* (B, D, F, H) animals expressing DAF-16a::GFP *(zIs356)*. DAF-16a::GFP (green) is present on vesicles in both wild-type and *tbc-2(tm2241)* intestinal cells (A and B) that are positive for autofluorescence (blue) present in the the endolysosomal system (E and F). Corresponding DIC (C and D) and merged (G and H) images are shown. A representative vesicle is shown (arrow head) and the two nuclei of the binucleate cell are marked (n). Note that DAF-16a::GFP is excluded from the large nucleoli (A). (I-J) Grouped bar graphs quantifying the percentage of wild-type (I) and *tbc-2(tm2241)* (J) animals with 0, 1–10, 11–50 or >50 DAF-16a::GFP *(zIs356)* positive vesicles at the different larval

stages (L1-4) or 1 and 3 day old adults (A1 and A3). Raw data is available in S1 Data. (K) A Tukey boxplot of the nuclear intensity in artificial units (a.u.) of DAF-16a::GFP in *tbc-2(tm2241)* intestinal cells with and without DAF-16a::GFP positive vesicles. Raw data is available in S1 Data. *n*, total number of animals *** $P<0.001$ in an unpaired t test (Prism 8). Scale bar (A), 10μm.

https://doi.org/10.1371/journal.pgen.1010328.g001

and not the GFP tag. Of note, we found that GFP expression in the *tbc-2* background was visibly stronger than in wild type (S3B–S3E Fig), consistent with *vha-6* ranking amongst the top downregulated DAF-16-responsive genes [31] and consistent with TBC-2 facilitating DAF-16 nuclear localization.

To determine if endogenous DAF-16 localizes to vesicles we analyzed *daf-16(hq23)*, a DAF-16::GFP line generated by CRISPR/Cas9 genome editing [32], and found that endogeneously tagged DAF-16 localized to vesicles in both wild type and *tbc-2(tm2241)* mutants (S2A–S2F Fig). To determine if the GFP/RFP tag is driving vesicular localization of DAF-16 we analyzed two *daf-16* alleles endogenously tagged with evolutionarily distant mNeongreen and mKate2 fluorescent proteins [33,34]. We found that DAF-16::mNG and DAF-16::mK2 both localized to intestinal vesicles in wild-type animals (Fig 2). DAF-16 positive vesicles are marked with arrowheads and are distinct from intestinal autofluorescence in the other fluorescence channels. Furthermore, the percent wild-type and *tbc-2(tm2241)* animals with endogenous DAF-16::mNG vesicles were comparable to that of the overexpressed DAF-16a::GFP (Fig 2I). Therefore, DAF-16 localization to vesicles is not due to overexpression and unlikely to be an artifact of the fluorescent tag.

The finding that DAF-16 localizes to enlarged vesicles in *tbc-2* mutants and that DAF-16 vesicles contain autofluorescent material (Figs 1E–1H, 2E and 2F), a hallmark of intestinal endolysosomes [35–37], suggested that DAF-16 vesicles are endosomal. To determine if the DAF-16 vesicles are endosomes, we co-expressed DAF-16a::GFP with RFP::RAB-5, an early endosomal marker, or with mCherry::RAB-7, a late endosomal marker [38–40]. We found that in wild-type animals, DAF-16a::GFP localizes to a subset of RAB-5 and RAB-7-positive endosomes (Fig 3A–3F). Thirty percent of DAF-16a::GFP vesicles were RAB-5 positive (n = 959) while 5% were RAB-7 positive (n = 365). Furthermore, we tested the genetic requirements for *rab-5* and *rab-7* for DAF-16 localization by RNAi. We found that *rab-5(RNAi)* and *rab-7(RNAi)* knockdown significantly decreased the number of wild-type and *tbc-2(tm2241)* animals with DAF-16a::GFP vesicles (Fig 3G and 3H). Together, these data are consistent with DAF-16 localizing to a sub-population of endosomes or endosome-like vesicles in the intestinal cells. It further implicates endosomal regulators TBC-2, RAB-5 and RAB-7 as regulators of DAF-16.

Acute starvation suppresses DAF-16 localization to endosomes

Nuclear localization of DAF-16 is modulated by nutrient availability. As such, starvation promotes DAF-16 cytoplasmic-to-nuclear shuttling [28]. To determine if endosomal DAF-16 can translocate to the nucleus, we tested the effect of acute starvation on DAF-16a::GFP localization to endosomes. We found that starvation strongly suppressed the localization of DAF-16 to endosomes in both wild type and *tbc-2(tm2241)* mutants (Figs 4A and S4). Upon re-feeding, DAF-16 relocalized to endosomes after 1–2 hours, in both wild type and *tbc-2(tm2241)* mutants. Thus, DAF-16 localization on endosomal membranes is regulated by nutrient availability.

Insulin/IGF signaling regulates DAF-16 localization to endosomes

To determine if IIS regulates DAF-16 localization to endosomes we analyzed the effect of disrupting IIS on DAF-16a::GFP localization (see Fig 4B for reference). Firstly, we analyzed a

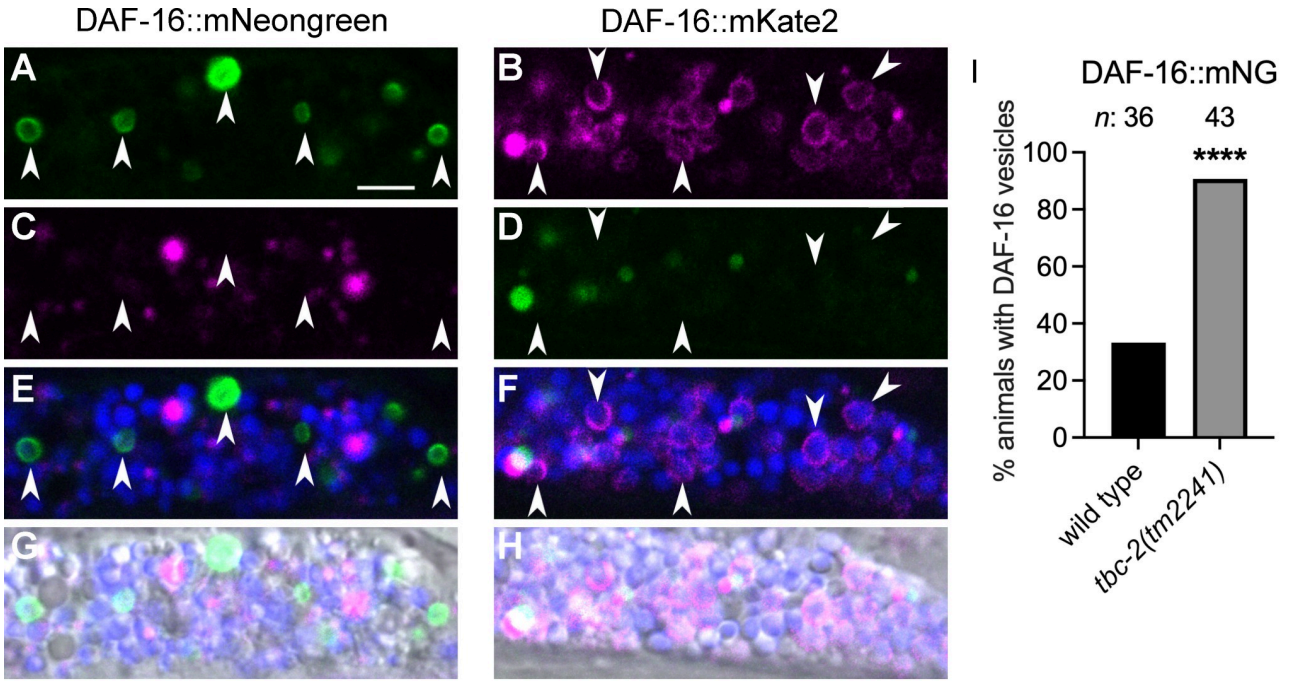

Fig 2. Endogenously tagged DAF-16::mNeongreen and DAF-16::mKate2 localize to vesicles. Representative confocal and differential interference contrast (DIC) images of intestinal cells of *daf-16(ot853[daf-16::linker::mNeongreen::3xFlag::AID])* (A,C,E,G) and *daf-16(ot821[daf-16::mKate2::3xFlag])* (B,D,F,H). Arrows mark DAF-16::mNeongreen positive vesicles in the green channel (A) that are distinct from autofluorescence in the red (C) and blue channels shown as a merge (E). Arrows mark DAF-16::mKate2 positive vesicles in the red channel (B) that are distinct from autofluorescence in the green (D) and blue channels shown as a merge (F). For additional context the fluorescent channels were merged with their corresponding DIC image (G and H). Bar graphs displaying the percent wild-type and *tbc-2(tm2241)* animals with DAF-16::mNG positive vesicles (I). Raw data is available in S1 Data. Fisher's exact test (graphpad.com) was used to determine the statistical difference between conditions. *n*, total number of animals. **** $P<0.0001$. Scale bar (A), 5μm.

https://doi.org/10.1371/journal.pgen.1010328.g002

hypomorphic mutant of the insulin/IGF receptor, *daf-2(e1370)*, in which IIS is reduced, particularly at higher temperatures [41]. We compared DAF-16a::GFP localization in three independent *daf-2(e1370)* strains at 15˚C and shifted overnight to 25˚C to enhance disruption of DAF-2. All three showed a significant reduction in the number of DAF-16 positive vesicles at 25˚C, while the wild-type strain did not (Fig 4C), indicating that DAF-2 promotes DAF-16 localization to endosomes.

DAF-18, the homolog of human tumor suppressor protein PTEN, acts as a negative regulator of the IIS pathway counteracting AGE-1 PI3K signaling by dephosphorylating the 3'phosphate on the $PI(3,4,5)P_3$ converting it to $PI(4,5)P_2$ [42]. We analyzed DAF-16a::GFP localization in the *daf-18* reference allele, *e1375*. We generated three independent *daf-18 (e1375); zIs356* strains, but only two strains had increased endosome localization of DAF-16. However, combined data from the three strains had a statistically significant increase in the number of animals with DAF-16 endosomes (Fig 4D). Since *daf-18(e1375)* is possibly a non-null allele, we analyzed a deletion allele, *daf-18(ok480)*. We found that five independent *daf-18 (ok480); zIs356* strains had more DAF-16 endosomes than wild type that when combined was statistically significant (Fig 4D). Since DAF-16 endosome localization is mildly increased in the background of two distinct *daf-18* alleles, it is consistent with increased IIS causing an increase in DAF-16 localization to endosomes.

C. elegans AKT-1 and AKT-2 function upstream of, and can phosphorylate, DAF-16 [43,44]. The SGK-1 Serum Glucorticoid Kinase homolog interacts with AKT kinases and has been shown to regulate DAF-16 nuclear localization [44]. We tested which of these kinases

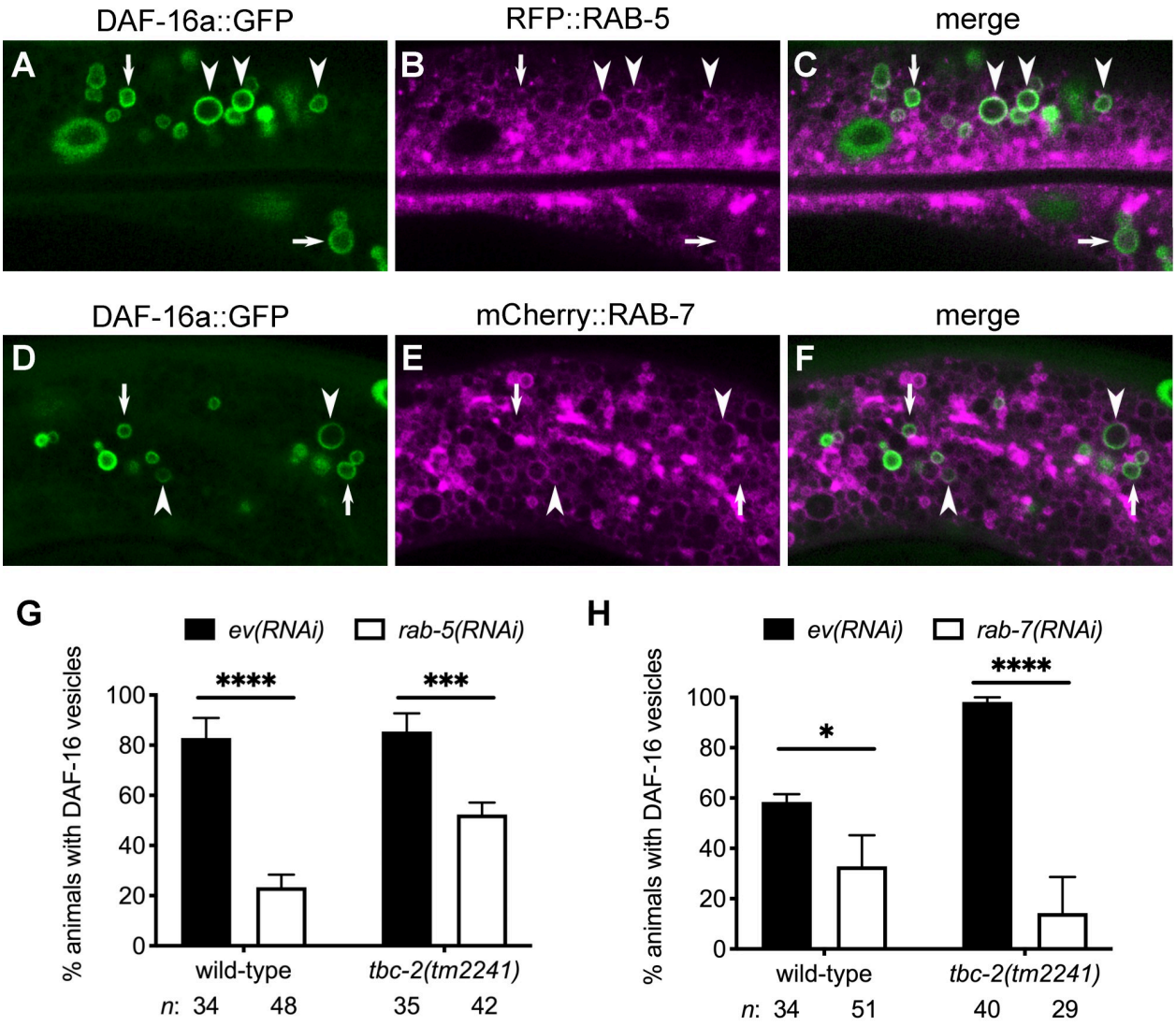

Fig 3. RAB-5 and RAB-7 GTPases promote DAF-16 FOXO localization to endosomes. (A-F) Representative confocal images of the intestinal cells of animals expressing DAF-16a::GFP (*zIs356)* (green) and either RFP::RAB-5 (*pwIs480*) (A-C) or mCherry::RAB-7 (*pwIs429*) (magenta) (D- F). Arrowheads mark examples of vesicles positive for both DAF-16a::GFP and either RFP::RAB-5 or mCherry::RAB-7. Arrows mark examples of DAF-16a::GFP vesicles that are not positive for either RFP::RAB-5 or mCherry::RAB-7. (G and H) Bar graphs displaying the mean (and SEM) of the percent wild-type and *tbc-2(tm2241)* animals with DAF-16a::GFP (*zIs356*) vesicles fed bacteria expressing control empty vector (ev) RNAi (black bars) compared to animals fed *rab-5(RNAi)* or *rab-7(RNAi)* (white bars) from three independent experiments. Raw data is available in S1 Data. Fisher's exact test (graphpad.com) was used to determine the statistical difference between conditions. *n*, total number of animals. * $P<0.05$, *** $P<0.001$, **** $P<0.0001$.

https://doi.org/10.1371/journal.pgen.1010328.g003

might regulate DAF-16 localization to endosomes. We found that animals with an *akt-2 (ok393)* deletion mutation, there was an insignificant decrease in DAF-16 endosomal localization in two independent strains (Fig 4E). However, in *akt-1*(*RNAi)* animals, we observed a significant decrease in DAF-16 endosomal localization where DAF-16 localized mainly to the nucleus, compared to the control animals in three independent experiments (Fig 4F). Neither an *sgk-1(ok538)* deletion nor an *sgk-1(ft15)* gain-of-function allele affected DAF-16 localization to endosomes [44,45](Fig 4G). Therefore, AKT-1 is the main kinase regulating DAF-16 localization to endosomes.

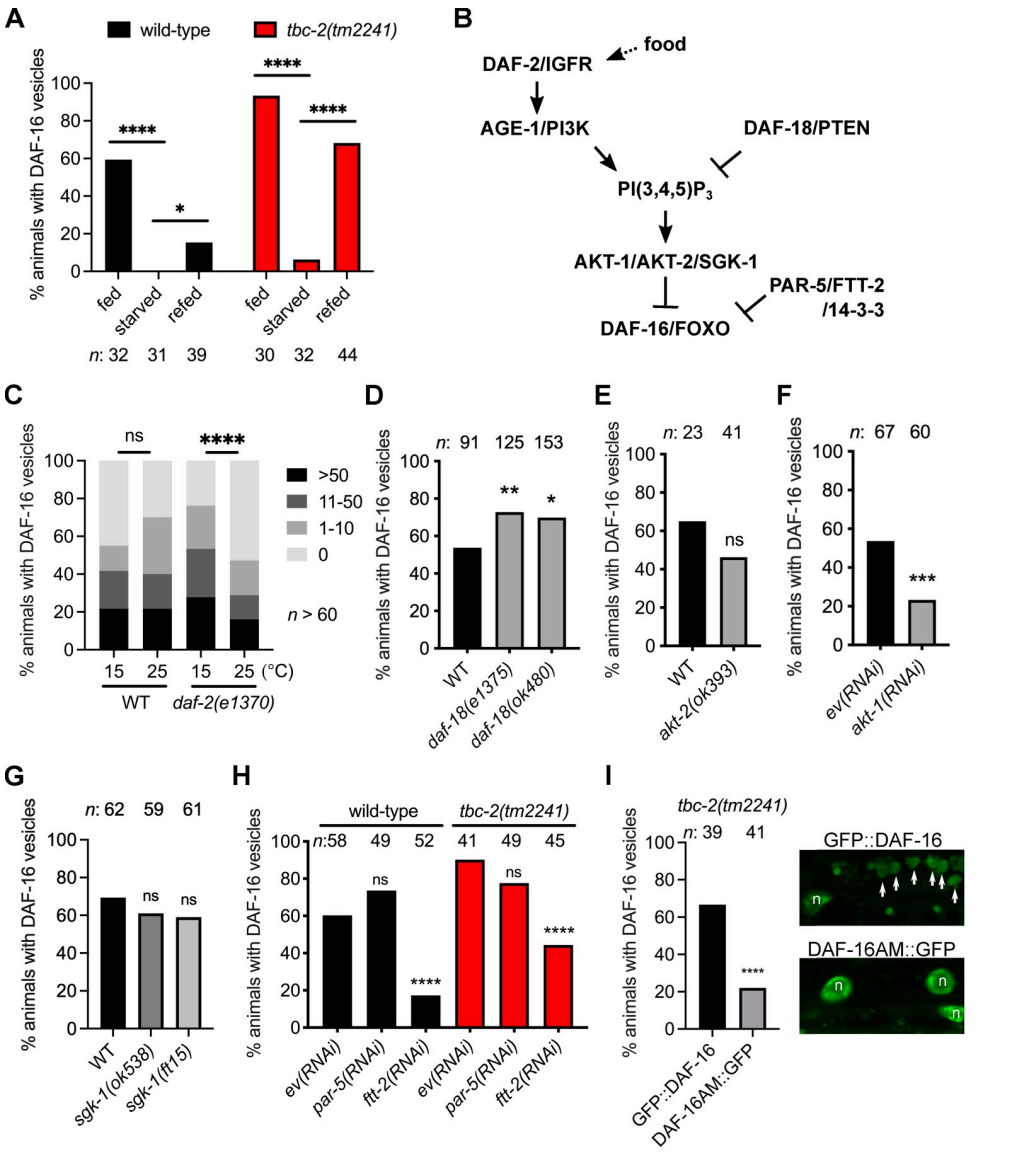

Fig 4. DAF-16 FOXO endosome localization is regulated by IIS and nutrient availability. (A) Bar graphs of the percent wild-type (black) and *tbc-2(tm2241)* (red) animals with DAF-16a::GFP (*zIs356*) vesicles in fed animals, animals starved between 4 and 5 hours and starved animals that have been refed for 1 to 2 hours. (B) Diagram of IIS-mediate regulation of DAF-16/FOXO. (C) Grouped bar graphs quantifying the percentage of wild-type and *daf-2(e1370)* L4 larvae (cumulative data from 3 independent strains) with 0, 1–10, 11–50 or >50 DAF-16a::GFP *(zIs356)* positive vesicles at 15˚C or shifted overnight to 25˚C. (D) Bar graphs of percent wild-type and *daf-18(e1375)* (cumulative data from 3 independent strains) and *daf-18(ok480)* (cumulative data from 5 independent strains) with DAF-16a::GFP (*zIs356*) vesicles. (E) Bar graphs of percent wild-type and *akt-2(ok393)* (cumulative data from 2 independent strains) with DAF-16a::GFP (*zIs356*) vesicles. (F) Bar graphs of percent wild-type animals treated with control empty vector RNAi and *akt-1(RNAi)* with DAF-16a::GFP (*zIs356*) vesicles. (G) Bar graphs of percent wild-type, *sgk-1(ok538)* and *sgk-1(ft15)* with DAF-16a::GFP (*zIs356*) vesicles. (H) Bar graphs of the percent wild-type (black) and *tbc-2(tm2241)* (red) animals fed control empty vector RNAi, *par-5(RNAi)* and *ftt-2(RNAi)* with DAF-16a::GFP (*zIs356*) vesicles. (I) Bar graph of the precent *tbc-2(tm2241)* animals with GFP::DAF-16a (*muIs71*) or DAF-16a^{AM}::GFP *(muIs113)*-positive vesicles. Raw data is available in S1 Data. Representative images of GFP::DAF-16a (*muIs71*) (top) and DAF-16a^{AM}:: GFP *(muIs113)* (bottom) are shown. GFP::DAF-16a vesicles (arrows) and the nuclei (n). Fisher's exact test (graphpad.com) was used to determine the statistical difference between conditions. *n*, total number of animals. ns, not significant, * $P<0.05$, ** $P<0.01$, *** $P<0.001$, **** $P<0.0001$.

https://doi.org/10.1371/journal.pgen.1010328.g004

Phosphorylation of FOXO proteins by Akt creates binding sites for 14-3-3 proteins, which promote cytoplasmic retention of FOXO [46]. *C. elegans* has two genes that encode for 14-3-3 proteins that interact with DAF-16, *par-5* and *ftt-2* [47–49]. We found that *ftt-2(RNAi)*, but not *par-5(RNAi)*, suppressed the localization of DAF-16 to endosomes (Fig 4H), suggesting that FTT-2 regulates DAF-16 endosomal localization.

To determine if AKT phosphorylation regulates DAF-16 localization to endosomes we tested if DAF-16a^{AM}::GFP *muIs113*, in which the four consensus AKT phosphorylation sites (T54A, S240A, T242 and S314A) are mutated to alanine [29], could still localize to vesicles in *tbc-2(tm2241)* mutants. Since the expression levels are lower than DAF-16a::GFP *zIs356*, we used GFP::DAF-16a *muIs71* with comparable expression levels as control (S5 Fig). We found that the number of *tbc-2(tm2241)* animals with DAF-16a^{AM}::GFP positive vesicles was significantly less than the GFP::DAF-16a control (Fig 4I). Together, these data demonstrate that IIS regulates endosomal DAF-16 through AKT-1 specific phosphorylation and FTT-2 14-3-3.

TBC-2 is required for lifespan extension and increased fat storage of *daf-2 (e1370)* mutants

To determine if the increased endosomal localization of DAF-16 seen in *tbc-2* mutants affects DAF-16 activity, we tested if TBC-2 regulates adult lifespan. We found that the *tbc-2(sv41)* and *tbc-2(tm2241)* deletion alleles had similar lifespans as compared to wild type (Fig 5A and 5B). As expected, *daf-2(e1370)* animals lived significantly longer than wild type. We found that both *tbc-2* alleles significantly shortened the lifespan of *daf-2(e1370)* animals (Fig 5A and 5B). Thus, TBC-2 is not required for normal lifespan, but is partly required for the extended lifespan of *daf-2(e1370)* mutants.

To assess TBC-2's contribution to other *daf-2* mutant phenotypes, we tested whether TBC-2 is required for the increased fat storage of *daf-2(e1370)* mutants. Consistent with previous findings we found that *daf-2(e1370)* had significantly more fat than wild-type animals as determined by Nile Red and Oil Red O staining of fixed L4 larvae [50,51] (Fig 5C–5F). We found that *tbc-2 (tm2241)* larvae had less fat than wild type with Nile Red staining, but not with Oil Red O staining (Fig 5D and 5F). This difference might reflect the lower sensitivity of Oil Red O for quantifying lipid abundance as compared to Nile Red [52]. Interestingly, we found that *tbc-2(tm2241)* significantly suppressed the *daf-2(e1370)* increased lipid staining by both Nile Red and Oil Red O (Fig 5C–5F). Thus, TBC-2 is required for the increased fat storage of *daf-2(e1370)* mutants.

The fact that TBC-2 is required for the increased longevity and increased fat storage of *daf-2(e1370)* mutants suggests that TBC-2 could be a negative regulator of IIS. Therefore, we tested if *tbc-2* mutants regulate DAF-16 target gene expression in *daf-2(e1370)* animals. We used qRT-PCR to measure the expression of DAF-16 target genes in wild type, *daf-2(e1370)*, *tbc-2* mutants and *tbc-2; daf-2* double mutants. Consistent with previous reports, the expression of six of the DAF-16 target genes were upregulated in *daf-2(e1370)* animals (Fig 6) [31,53–55]. While *tbc-2(tm2241)* and *tbc-2(sv41)* did not appreciably alter DAF-16 target gene expression relative to wild type, both reduced the expression of *sod-3*, *dod-3*, *gpd-2* and *icl-1* in *daf-2 (e1370)* mutants, while *mtl-1* and *ftn-1* were not significantly decreased (Fig 6). The fact that TBC-2 was required for the increased expression of four of six DAF-16 target genes with elevated expression in *daf-2(e1370)* mutants suggests a more specific role for TBC-2 in regulating DAF-2 to DAF-16 signaling.

Discussion

Endosome trafficking and signal transduction are intimately linked processes regulating signal propagation, specificity and attenuation [9,56]. However, there remains a large knowledge gap

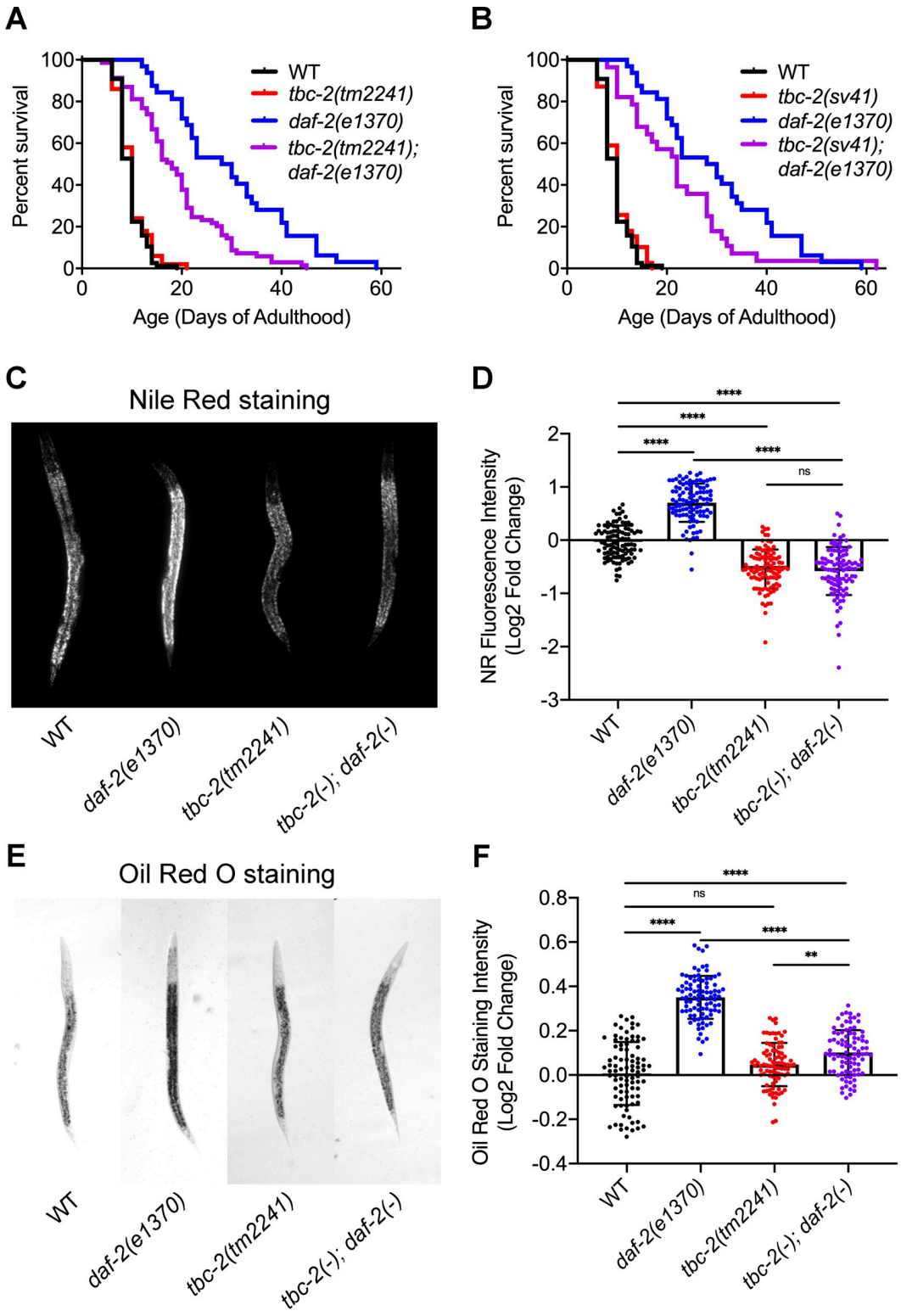

Fig 5. TBC-2 is required for full lifespan extension and increased fat storage resulting from decreased insulin/IGF signaling. (A,B) Percent survival curve of adult animals of wild-type and *daf-2(e1370)* with either *tbc-2(tm2241)* and *tbc-2(tm2241); daf-2(e1370)* (A) or *tbc-2(sv41)* and *tbc-2(sv41); daf-2(e1370)* (B) genotypes. The survival of all strains are statistically different from *daf-2(e1370)* animals as determined by a Mantel-Cox log-rank test: *tbc-2(tm2241); daf-2(e1370)* ($P<0.001$) and *tbc-2(sv41); daf-2(e1370)* ($P = 0.0314$). Cumulative data from three independent replicates of 50 young adults for a total of 150. (C,E) Representative

images of wild-type, *daf-2(e1370)*, *tbc-2(tm2241)* and *tbc-2(tm2241); daf-2(e1370)* L4 hermaphrodites fixed and stained with Nile Red (C) or Oil Red O (E). (D,F) Log2 fold change in Nile Red (NR) fluorescence intensity (D) or Oil Red O staining intensity (F) comparing wild-type, *daf-2(e1370)*, *tbc-2(tm2241)* and *tbc-2(tm2241); daf-2(e1370)* fixed L4 hermaphrodites. Raw data is available in S1 Data. Statistical analysis was done using a student's t-test with a one way analysis of variance (ANOVA). ns, not significant. ** $P < 0.01$, **** $P < 0.0001$.

https://doi.org/10.1371/journal.pgen.1010328.g005

in the spatial regulation of cell signaling and where downstream transcription factors are regulated. We identified a previously unknown localization for the DAF-16 FOXO transcription factor on endosomes in *C. elegans*. Endosome localization is limited by the TBC-2 Rab GAP. Loss of *C. elegans* TBC-2 results in increased endosomal localization of DAF-16 at the expense of nuclear localization. As such, *C. elegans* TBC-2 is partly required for several *daf-2 IGFR* mutant phenotypes including lifespan extension, increased fat storage, and increased DAF-16 target gene expression that result from DAF-16 nuclear translocation. DAF-16 endosome localization is largely dependent on IIS consistent with this being a phosphorylated, inactive pool of DAF-16. Together our data show a role for the TBC-2 Rab GAP in regulating the balance of nuclear versus endosomal localization of the DAF-16 transcription factor.

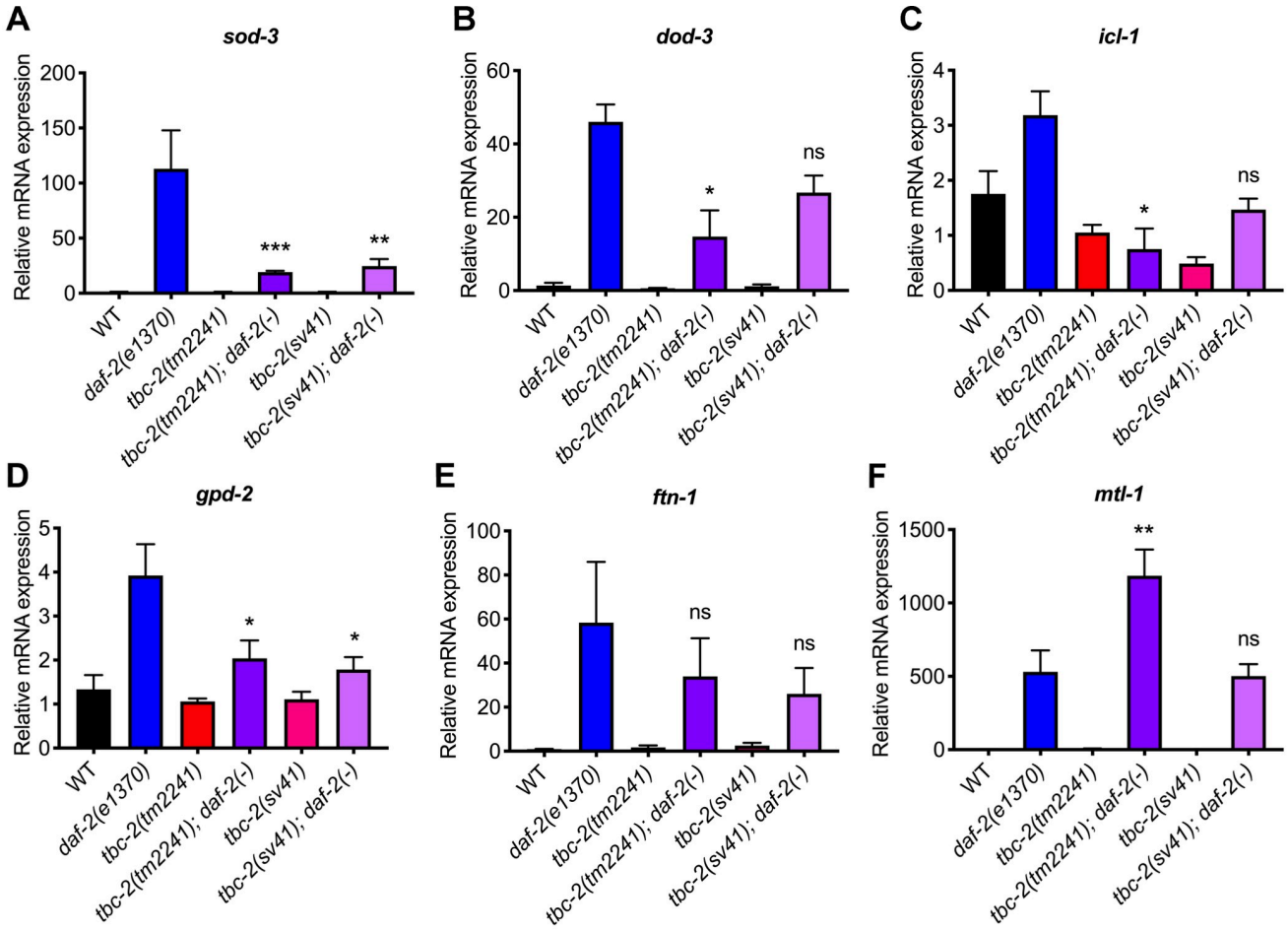

Fig 6. TBC-2 is required for the increased DAF-16 target gene expression resulting from decreased insulin/IGF signaling. Quantitative RT-PCR analysis of DAF-16 target gene expression in wild type, *daf-2(e1370)*, *tbc-2(tm2241)*, *tbc-2(tm2241); daf-2(e1370)*, *tbc-2(sv41)*, and *tbc-2(sv41); daf-2(e1370)*. Statistical analysis was performed using an Ordinary one-way ANOVA–Tukey's multiple comparisons test. Shown are comparisons of *tbc-2(tm2241); daf-2(e1370)* and *tbc-2(sv41); daf-2(e1370)* versus *daf-2(e1370)* single mutants. Raw data is available in S1 Data. ns, not significant. * $P < 0.05$, ** $P < 0.01$, *** $P < 0.001$.

https://doi.org/10.1371/journal.pgen.1010328.g006

DAF-16 localizes to endosomes

We were surprised to find that DAF-16 FOXO localizes to a subset of RAB-5 and RAB-7 endosomes in wild-type animals. Many studies have used DAF-16 cytoplasmic versus nuclear localization to assess IIS activity under various conditions. We assume that DAF-16 positive endosomes were not discovered earlier as nuclear translocation can be assessed at low magnification where DAF-16 positive endosomes are not apparent, and DAF-16 positive endosomes are not present in every cell or every animal. Furthermore, we first took notice of DAF-16 positive endosomes in the *tbc-2* mutant background where they are more prominent. These are likely not an artefactual consequence of overexpression, as we see these vesicles in the endogenously tagged *daf-16*::*GFP* and we do not see similar vesicles in a GFP overexpression strain. DAF-16::mNG and DAF-16::mK2 also localize to vesicles indicating that membrane localization is unlikely to be an artifact of the GFP tag. Additionally, DAF-16-vesicles are regulated by IIS.

Many components of the IIS pathway localize to endosomes in mammalian cells including active insulin receptor and downstream signaling components such as PI3K, Akt, PTEN and 14-3-3 proteins [9,11,15,57–61]. In the case of Akt and PTEN, both have demonstrated roles in regulation of endosome trafficking independent of IIS [12,62–64]. On the other hand, the PI3Ks are Rab5 effectors and Rab5 has been shown to promote Akt activity on endosomes [60,61,65–67]. While endosomal localization of FOXO proteins has not been reported to the best of our knowledge, knockdown of Rab5 in mouse liver results in a strong increase in phosphorylated FOXO1 [68]. This is contrary to the finding that Rab5 promotes Akt phosphorylation [61,66], which could be a consequence of indirect regulation or suggest tissue-specific regulation. The fact that TBC-2 is a RAB-5 GAP is consistent with increased RAB-5 activity promoting DAF-16 localization on endosomes. This is further supported by the fact that *rab-5* and *rab-7* RNAi knockdown reduces the number of animals with DAF-16 vesicles in both wild type and *tbc*-2 mutants. Given the importance of RAB-5 for endosome trafficking, it is difficult to parse whether RAB-5 is promoting a platform for DAF-16 localization or if it also has a role in IIS.

We demonstrated that DAF-16 localized to a subset of RAB-5 and RAB-7 positive endosomes. Since RAB-5 and RAB-7 promote trafficking to the lysosome and promote receptor tyrosine kinase degradation, it is possible that DAF-16-positive endosomes are signaling endosomes, in which case we would expect other upstream signaling components might be present. Consistent with that hypothesis, knockdown of IIS reduces the number of animals with DAF-16 vesicles. However, when analyzing DAF-16 localization in *daf-2(e1370)* mutants at 15˚C vs. 25˚C, we find that while there is a reduction in the number of DAF-16 endosomes, these endosomes are noticeably fainter at 25˚C. This suggests that there are not necessarily less endosomes being generated, but rather less DAF-16 on the vesicles which may be inconsistent with these being signaling endosomes derived from DAF-2 internalization at the plasma membrane. On the other hand, the fact that Akt and 14-3-3 can localize to endosomes in mammalian cells [15,59,61] and that AKT-1 and FTT-2 promote DAF-16 localization to endosomes, suggests that these proteins might recruit DAF-16 onto endosomes rather than DAF-16 interacting directly with membranes. Future studies should test whether DAF-2 IGFR and downstream IIS components actively recruit DAF-16 to endosomes or whether IIS has a passive role. IIS inhibition of nuclear DAF-16 could result in increased DAF-16 in the cytoplasm where it can bind endosomes.

If these are not signaling endosomes, then what are the DAF-16 endosomes? Since RAB-5 and RAB-7 are also regulators of autophagy, so it is possible that these endosomes contribute to degradation of inactive excess DAF-16. There is precedent for selective autophagy in the

degradation of the GATA4 transcription factor [69]. Alternatively, these endosomes could serve as a reservoir of inactive DAF-16 that can be quickly mobilized if environmental stress is encountered. For example, we found that acute starvation is a potent regulator of DAF-16 endosome localization, even in the *tbc-2* mutant background.

We find it interesting that there is such variability within the population, and amongst the intestinal cells in a given animal, as to whether there will be DAF-16 positive endosomes or not. It suggests that each intestinal cell autonomously senses changes in IIS, or possibly other nutrient and stress sensing pathways, to regulate DAF-16 localization. Then, why is endosomal DAF-16 more prominent in *tbc-2* mutants? One explaination would be that the expansion of endosomal membranes in a *tbc-2* mutant create more storage space for inactive DAF-16. Another would be that IIS or other pathways are more active in *tbc-2* mutants, or some combination of the two. The fact that loss of IIS does not eliminate DAF-16 localization from endosomes suggests that additional signaling pathways could regulate DAF-16 endosome localization. GLP-1/Notch signaling in the germline regulates longevity in a DAF-16-dependent manner as well as DAF-16 nuclear translocation [70], and IIS post-translationally regulates GLP-1 signaling [71], thus it would be interesting to determine if DAF-16 localization to endosomes are regulated by GLP-1/Notch signaling and if TBC-2 regulates GLP-1 to DAF-16 target gene expression [72]. Additionally, AMPK, JNK and LET-363/mTor signaling regulate DAF-16 and could regulate DAF-16 localization to endosomes or be subject to regulation by TBC-2, particularly mTor which localizes to lysosomes [70,73–77].

A direct role for TBC-2 in regulating *daf-2(e1370) IGFR* mutant phenotypes

Our finding that *tbc-2* was required for the extended lifespan and increased fat storage of *daf-2 (e1370)* mutants suggests that TBC-2 might have a more specific role related to IIS. However, TBC-2 is not the first endosomal regulator required for lifespan extension of *daf-2(e1370)* mutants. *C. elegans* BEC-1, a homolog of human Beclin1, is a regulator of autophagy and endosome trafficking, and *bec-1* mutants accumulate large late endosomes in the intestinal cells [78–80]. Mutations in *bec-1* suppress the increased lifespan of *daf-2(e1370)*, and were reported to be required for the increased fat storage [78]. Similarly, other autophagy regulators, *atg-7* and *atg-12*, have been shown to be required for *daf-2* longevity [81]. An RNAi screen identified regulators of endosome to lysosome trafficking, including RAB-7, and components of the ESCRT and HOPS complexes as being required for the lifespan extension phenotypes of *daf-2 IGFR* mutants [82]. However, the mechanisms by which they regulate lifespan are not known. In *daf-2(e1370)* mutants, there is an increase in autophagy and lysosome function, both of which are required for the extended lifespan [78,83–85], consistent with increased stress resistance contributing to increased longevity. Since the human homologs of TBC-2 are implicated in autophagy [86–89], and *tbc-2* mutants accumulate autophagy protein LGG-1 (LC3/Atg8) in enlarged endosomes [19], it is possible that TBC-2 also regulates autophagy and thus *daf-2(-)* longevity. However, our findings that TBC-2 regulates DAF-16 nuclear vs. endosome localization and that TBC-2 is required for the DAF-16 target gene expression in *daf-2* mutants demonstrate that TBC-2 has a more direct role in IIS, as opposed to being required for downstream cellular responses. It will be interesting to test if TBC-2 regulates DAF-16-independent mechanisms of longevity as well as to determine if other endosome and autophagy-regulating genes can regulate DAF-16 localization to endosomes.

In conclusion, we demonstrate that the DAF-16 FOXO transcription factor localizes to endosomes. This endosomal localization of DAF-16 FOXO is regulated by both IIS and the TBC-2 Rab GAP. TBC-2 promotes the nuclear localization of DAF-16 FOXO, and this

localization has functional effects on both longevity and metabolism through modulation of DAF-16 target gene expression. Our data suggest that endosomes serve as an important location for DAF-16 FOXO transcription factor regulation, and suggest that endomembranes may function as a site of transcription factor regulation.

Methods

C. elegans genetics and strain construction

C. elegans strains were cultured as described in Wormbook (www.wormbook.org). The *C. elegans* N2 Bristol strain was the wild-type parent strain and HB101 *E. coli* strain was used as a food source. Both were obtained from the Caenorhabditis Genetic Center (CGC) as were many of the strains used in this study (S1 Table). New strains were constructed using standard methods and the presence of mutations were confirmed by PCR and DNA sequencing.

RNAi experiments

C. elegans RNAi feeding experiments were conducted essentially as described in [90]. RNAi feeding clones were obtained from the Ahringer RNAi library and confirmed by sequencing (S1 Table)[91,92]. The L4440 empty RNAi feeding vector transformed into HT115(DE3) was used as a negative control [93].

Microscopy

DAF-16 vesicular localization was analyzed in the intestinal cells of hermaphrodites. Hermaphrodite worms at the L4 stage were imaged alive at room temperature unless it is stated otherwise. Animals were picked and mounted onto 4% agarose pads, animals were anesthetized with levamisole.

Differential interference contrast (DIC) and fluorescent imaging were performed with an Axio Imager A1 compound microscope with a 100×1.3 NA Plan-Neofluar oil-immersion objective lens (Zeiss) and images were captured by using an Axio Cam MRm camera and AxioVision software (Zeiss). Confocal microscopy was performed on an Axio Observer Z1 LSM780 laser scanning confocal microscope with a 63×1.4 NA Plan-Apochromat oil-immersion objective lens (Zeiss) in a multi-track mode using an argon multiline laser (405 nm excitation for autofluoresence, 488 nm excitation for GFP and a 561/ 594 nm excitation for mCherry/RFP). Images were captured with a 32 channel GaAsP detector and ZEN2010 image software. Raw data was analyzed using Fiji (ImageJ) or Zen 2010 Lit programs, and images were modified by using Fiji (ImageJ).

To compare DAF-16 (*zIs356*) nuclear intensity in cells with or without DAF-16 vesicles, animals at L4 stage were imaged using an LSM780 scanning laser microscope. To ensure consistency, only the anterior most intestine cells were imaged. First, the nucleus of intestinal cells were focused under bright field and without changing the position, GFP, autofluoresence and bright field signals were imaged. Each animal was imaged using the same confocal settings. After data collection, each nucleus was categorized as a nucleus with adjacent DAF-16-positive vesicles or a nucleus without any DAF-16 positive vesicles. Total GFP intensity inside the nucleus was measured using Fiji (Image J) software. The nucleus is circled using DIC/Bright Field and autofluorescence channels as reference. Since intestinal cells have two nuclei per cells, if there are two nuclei within the focus, their GFP intensity is averaged for statistical analysis. Prism 8 (GraphPad) were used to graph the data and determine statistical analysis using an unpaired t-test.

Starvation-refeeding and temperature shift experiments

For starvation and refeeding experiments animals were synchronized at the L1 stage and grown on NGM plates with HB101 *E. coli* till the L4 stage. Then animals were collected washed 3 times for 5 mins with M9 buffer to remove bacteria in their gut. After the third wash animals were plated to regular NGM plates with or without HB101 *E. coli*, and incubated for 4–5 hours before scoring. Animals are scored for the presence of DAF-16::GFP-positive vesicles the intestine using an A1 Zeiss microscope. After 4h-5h of starvation, animals were harvested with M9 buffer from the starved plates and washed once with M9 buffer and plated to NGM plates with HB101 *E. coli* and incubated for 1–2 hours at 20˚C before scoring.

Life span analysis

Replicate strains were maintained for several generations prior to beginning the lifespan assays which were conducted at 20˚C. For each strain 25 young adult hermaphrodites were picked to two NGM plates without FUDR seeded with HB101 *E. coli* for three independent replicates totaling 150 animals. Strains were coded and scored blindly to reduce bias. Animals were transferred to fresh NGM plates to avoid contamination and getting crowded out by their progeny. Animals were scored every 2–3 days and were considered dead when they stop exhibiting spontaneous movement and fail to move in response to 1) a gentle touch of the tail, 2) a gentle touch of the head, and 3) gently lifting the head. Animals that die of unnatural causes (internal hatching of embryos, bursting, or crawling off the plate) are omitted. Graphs and statistics were done using Graphpad Prism. None of the strains used in the lifespan assays carry the *fln-2(ot611)* mutation found in a N2 male stock strain and found to extend median lifespan [94,95].

Fat staining

L4 animals were fixed for staining with Nile Red (Invitrogen) or Oil Red O (Sigma-Aldrich) as previously described [52]. Imaging and analysis was done as previously described [96]. Graphs and statistics were done using Graphpad Prism.

Quantitative real-time RT-PCR

C. elegans RNA was isolated from young adults maintained at 15˚C using TRIZOL reagent (Invitrogen). 1 ug of RNA was reverse transcribed into cDNA using the High-Capacity cDNA Reverse Transcriptase Kit (Applied Biosystems). Quantitative real-time PCR was performed using 1 μl of the cDNA preparation with SYBR-Green Reagents and a Vii7 qPCR analyzer (Applied Biosystems). Each DAF-16 target gene was amplified using PCR primers as described in [97] and compared to *act-3* (S1 Table).

Statistical analysis

Statistical analysis was carried out using GraphPad Prism software. For the analysis of two groups, a student t test was performed using two-tailed distribution for analysis involving two groups of samples. Fishers' exact test was used for comparing groups of four. For each analysis, $P<0.05$ was considered as significant.

Supporting information

S1 Fig. DAF-16::GFP localizes to vesicles in wild-type and *tbc-2* animals at all post-embryonic developmental stages and in wild-type males. (A) Bar graph of the percent animals with DAF-16a::GFP *(zIs356)* positive vesicles in the intestinal cells at larval stages L1-L4 and young

adults of wild-type and *tbc-2(tm2241)* animals at 20˚C. Fisher's exact test (graphpad.com) was used to determine that there is a significant increase the number of *tbc-2(tm2241)* animals with DAF-16a::GFP as compared to wild type at each developmental stage (L1: $P<0.05$, L2-adult: $P<0.0001$, n = 23 to 47 animals). (B) Bar graph of the percent *zIs356*/+ L4/young adult hermaphrodites and males with DAF-16a::GFP positive vesicles. Raw data is available in S1 Data. ns, not significant, n = 47–50 animals.
(TIF)

S2 Fig. DAF-16 FOXO localizes to vesicles in intestinal cells. Representative confocal and differential interference contrast (DIC) images of intestinal cells of wild-type (A-C, G-I, M-O and S-U) and *tbc-2(tm2241)* (D-F, J-L, P-R and V-X) animals expressing DAF-16::GFP *daf-16 (hq23)* (A-F), *muIs71* GFP::DAF-16a (G-L), *lpIs12* DAF-16a::RFP (M-R) and *lpIs14* DAF-16f::GFP (S-X). Endogenously tagged DAF-16::GFP *daf-16(hq23)* is present on vesicles in both wild-type and *tbc-2(tm2241)* intestinal cells (A and D arrowheads). Arrows mark bright autofluorescent lysosome-related organelles that bleed through the GFP channel in these lower expressing strains. Vesicular localization of GFP::DAF-16a (G and J), DAF-16a::RFP (M and P) and DAF-16f::GFP (S and V) was only seen in *tbc-2(tm2241)* animals and not visible in wild-type backgrounds. Scale bars (A, G, M, S), 10**μ**m.
(TIF)

S3 Fig. GFP localization and expression in wild-type and *tbc-2* mutants. (A) Grouped bar graph quantifying the number of wild-type and *tbc-2(tm2241)* L4 larvae with 0, 1–10, 11–50 or >50 GFP *(vhEx1[Pvha-6::GFP])* positive vesicles or aggregates (aggregates were included in the analyses which are not often seen with DAF-16a::GFP). Raw data is available in S1 Data. (B-E) DIC and epifluorescence images of wild-type and *tbc-2(tm2241)* (B,C) as well as wild-type and *tbc-2(sv41)* (D,E) animals expressing GFP under an intestine specific promoter, *vhEx1 [Pvha-6::GFP]*. White and yellow arrowheads mark the anterior of the intestine of wild-type and *tbc-2* mutant animals, respectively. Both *tbc-2* mutants have increased GFP expression as compared to wild-type animals. *tbc-2* mutants were distinguished from wild-type by the presence of enlarged vesicles using the 100X objective (not shown).
(TIF)

S4 Fig. Endosomal DAF-16 is suppressed by acute starvation. Epifluorescence (A,C,E,G,I,K) and DIC (B,D,F,H,J,L) images of wild-type (A-F) and *tbc-2(tm2241)* (G-L) animals under fed (A,B,G,H), 4–5 hours of starvation (C,D,I,J) and after 1–2 hours of refeeding (E,F,K,L). Scale bar (A), 10μm.
(TIF)

S5 Fig. GFP::DAF-16 and DAF-16AM::GFP have similar expression levels. Bar graph depicting the mean pixel intensities of GFP fluorescence in the intestine of QR508 *tbc-2 (tm2241); muIs71[GFP::DAF-16]* and QR697 *tbc-2(tm2241); muIs113[DAF-16AM::GFP]* animals. Raw data is available in S1 Data. The difference was determined to be not significant (ns) in an unpaired t test.
(TIF)

S1 Table. List of key resources used in this study including bacterial strains, *C. elegans* strains, RNAi-feeding clones, and oligonucleotides.
(DOCX)

S1 Data. Raw numbers and statistical analyses summarized in the bar graphs.
(XLSX)

Acknowledgments

We thank Ali Fazlollahi for technical assistance, Meera Sundaram (University of Pennsylvania) for comments and suggestions, Simon Wing, Richard Roy and Monique Zetka (McGill University) for reagents, Aimee Kao (UCSF) for *muIs113*, Patrick Hu (Vanderbilt University) for the *sgk-1* strains as well as Yanping Zhang, Wenhong Zhang and Meng-Qiu Dong (National Institute of Biological Sciences, Beijing) for generously sharing *daf-16(hq23)* ahead of publication. We thank Wormbase for information on genes and mutations. Some deletion mutations used in this study were provided by the National BioResource Project (Japan) and the International *C. elegans* Gene Knockout Consortium at the Oklahoma Medical Research Foundation, which is funded by the National Institutes of Health (NIH); and the University of British Columbia, which is funded by the Canadian Institute for Health Research (CIHR), Genome Canada, Genome B.C., the Michael Smith Foundation, and the NIH. Some strains were provided by the CGC, which is funded by NIH Office of Research Infrastructure Programs (P40 OD010440).

Author Contributions

Conceptualization: İçten Meraş, Benjamin Wiles, Christian E. Rocheleau.

Data curation: Christian E. Rocheleau.

Formal analysis: İçten Meraş, Laëtitia Chotard, Thomas Liontis, Zakaria Ratemi, Benjamin Wiles, Jeremy M. Van Raamsdonk, Christian E. Rocheleau.

Funding acquisition: Jeremy M. Van Raamsdonk, Christian E. Rocheleau.

Investigation: İçten Meraş, Laëtitia Chotard, Thomas Liontis, Zakaria Ratemi, Benjamin Wiles, Jung Hwa Seo, Christian E. Rocheleau.

Project administration: Christian E. Rocheleau.

Supervision: Jeremy M. Van Raamsdonk, Christian E. Rocheleau.

Writing – original draft: İçten Meraş, Christian E. Rocheleau.

Writing – review & editing: İçten Meraş, Laëtitia Chotard, Thomas Liontis, Benjamin Wiles, Jeremy M. Van Raamsdonk, Christian E. Rocheleau.

References

1. Murphy CT, Hu PJ. Insulin/insulin-like growth factor signaling in C. *elegans*. WormBook. 2013:1–43. https://doi.org/10.1895/wormbook.1.164.1 PMID: 24395814
2. Accili D, Arden KC. FoxOs at the crossroads of cellular metabolism, differentiation, and transformation. Cell. 2004; 117(4):421–6. https://doi.org/10.1016/s0092-8674(04)00452-0 PMID: 15137936
3. Barthel A, Schmoll D, Unterman TG. FoxO proteins in insulin action and metabolism. Trends Endocrinol Metab. 2005; 16(4):183–9. https://doi.org/10.1016/j.tem.2005.03.010 PMID: 15860415
4. Greer EL, Brunet A. FOXO transcription factors at the interface between longevity and tumor suppression. Oncogene. 2005; 24(50):7410–25. https://doi.org/10.1038/sj.onc.1209086 PMID: 16288288
5. Riddle DL, Swanson MM, Albert PS. Interacting genes in nematode dauer larva formation. Nature. 1981; 290(5808):668–71. https://doi.org/10.1038/290668a0 PMID: 7219552
6. Kenyon C, Chang J, Gensch E, Rudner A, Tabtiang R. A *C. elegans* mutant that lives twice as long as wild type. Nature. 1993; 366(6454):461–4. https://doi.org/10.1038/366461a0 PMID: 8247153
7. Ogg S, Paradis S, Gottlieb S, Patterson GI, Lee L, Tissenbaum HA, et al. The Fork head transcription factor DAF-16 transduces insulin-like metabolic and longevity signals in *C.* elegans. Nature. 1997; 389 (6654):994–9. https://doi.org/10.1038/40194 PMID: 9353126

8. Lin K, Dorman JB, Rodan A, Kenyon C. *daf-16*: An HNF-3/forkhead family member that can function to double the life-span of *Caenorhabditis elegans*. Science. 1997; 278(5341):1319–22. https://doi.org/10.1126/science.278.5341.1319 PMID: 9360933

9. Bergeron JJ, Di Guglielmo GM, Dahan S, Dominguez M, Posner BI. Spatial and Temporal Regulation of Receptor Tyrosine Kinase Activation and Intracellular Signal Transduction. Annual review of biochemistry. 2016; 85:573–97. https://doi.org/10.1146/annurev-biochem-060815-014659 PMID: 27023845

10. Baass PC, Di Guglielmo GM, Authier F, Posner BI, Bergeron JJ. Compartmentalized signal transduction by receptor tyrosine kinases. Trends Cell Biol. 1995; 5(12):465–70. https://doi.org/10.1016/s0962-8924(00)89116-3 PMID: 14732031

11. Naguib A, Bencze G, Cho H, Zheng W, Tocilj A, Elkayam E, et al. PTEN functions by recruitment to cytoplasmic vesicles. Mol Cell. 2015; 58(2):255–68. https://doi.org/10.1016/j.molcel.2015.03.011 PMID: 25866245

12. Shinde SR, Maddika S. PTEN modulates EGFR late endocytic trafficking and degradation by dephosphorylating Rab7. Nature communications. 2016; 7:10689. https://doi.org/10.1038/ncomms10689 PMID: 26869029

13. Walz HA, Shi X, Chouinard M, Bue CA, Navaroli DM, Hayakawa A, et al. Isoform-specific regulation of Akt signaling by the endosomal protein WDFY2. J Biol Chem. 2010; 285(19):14101–8. https://doi.org/10.1074/jbc.M110.110536 PMID: 20189988

14. Schenck A, Goto-Silva L, Collinet C, Rhinn M, Giner A, Habermann B, et al. The endosomal protein Appl1 mediates Akt substrate specificity and cell survival in vertebrate development. Cell. 2008; 133(3):486–97. https://doi.org/10.1016/j.cell.2008.02.044 PMID: 18455989

15. Marat AL, Wallroth A, Lo WT, Muller R, Norata GD, Falasca M, et al. mTORC1 activity repression by late endosomal phosphatidylinositol 3,4-bisphosphate. Science. 2017; 356(6341):968–72. https://doi.org/10.1126/science.aaf8310 PMID: 28572395

16. Jungmichel S, Sylvestersen KB, Choudhary C, Nguyen S, Mann M, Nielsen ML. Specificity and commonality of the phosphoinositide-binding proteome analyzed by quantitative mass spectrometry. Cell Rep. 2014; 6(3):578–91. https://doi.org/10.1016/j.celrep.2013.12.038 PMID: 24462288

17. Settembre C, Fraldi A, Medina DL, Ballabio A. Signals from the lysosome: a control centre for cellular clearance and energy metabolism. Nat Rev Mol Cell Biol. 2013; 14(5):283–96. https://doi.org/10.1038/nrm3565 PMID: 23609508

18. Huotari J, Helenius A. Endosome maturation. EMBO J. 2011; 30(17):3481–500. https://doi.org/10.1038/emboj.2011.286 PMID: 21878991

19. Chotard L, Mishra AK, Sylvain MA, Tuck S, Lambright DG, Rocheleau CE. TBC-2 regulates RAB-5/RAB-7-mediated endosomal trafficking in *Caenorhabditis elegans*. Mol Biol Cell. 2010; 21(13):2285–96. https://doi.org/10.1091/mbc.e09-11-0947 PMID: 20462958

20. Libina N, Berman JR, Kenyon C. Tissue-specific activities of *C. elegans* DAF-16 in the regulation of lifespan. Cell. 2003; 115(4):489–502. https://doi.org/10.1016/s0092-8674(03)00889-4 PMID: 14622602

21. Li W, Zou W, Zhao D, Yan J, Zhu Z, Lu J, et al. *C. elegans* Rab GTPase activating protein TBC-2 promotes cell corpse degradation by regulating the small GTPase RAB-5. Development. 2009; 136(14):2445–55. https://doi.org/10.1242/dev.035949 PMID: 19542357

22. Sasidharan N, Sumakovic M, Hannemann M, Hegermann J, Liewald JF, Olendrowitz C, et al. RAB-5 and RAB-10 cooperate to regulate neuropeptide release in *Caenorhabditis elegans*. Proc Natl Acad Sci U S A. 2012; 109(46):18944–9. https://doi.org/10.1073/pnas.1203306109 PMID: 23100538

23. Liu O, Grant BD. Basolateral Endocytic Recycling Requires RAB-10 and AMPH-1 Mediated Recruitment of RAB-5 GAP TBC-2 to Endosomes. PLoS Genet. 2015; 11(9):e1005514. https://doi.org/10.1371/journal.pgen.1005514 PMID: 26393361

24. Sun L, Liu O, Desai J, Karbassi F, Sylvain MA, Shi A, et al. CED-10/Rac1 regulates endocytic recycling through the RAB-5 GAP TBC-2. PLoS Genet. 2012; 8(7):e1002785. https://doi.org/10.1371/journal.pgen.1002785 PMID: 22807685

25. Chotard L, Skorobogata O, Sylvain MA, Shrivastava S, Rocheleau CE. TBC-2 is required for embryonic yolk protein storage and larval survival during L1 diapause in *Caenorhabditis elegans*. PLoS One. 2010; 5(12):e15662. https://doi.org/10.1371/journal.pone.0015662 PMID: 21203392

26. Munoz MJ, Riddle DL. Positive selection of *Caenorhabditis elegans* mutants with increased stress resistance and longevity. Genetics. 2003; 163(1):171–80. https://doi.org/10.1093/genetics/163.1.171 PMID: 12586705

27. Baugh LR, Sternberg PW. DAF-16/FOXO regulates transcription of cki-1/Cip/Kip and repression of lin-4 during *C. elegans* L1 arrest. Curr Biol. 2006; 16(8):780–5. https://doi.org/10.1016/j.cub.2006.03.021 PMID: 16631585

28. Henderson ST, Johnson TE. *daf-16* integrates developmental and environmental inputs to mediate aging in the nematode *Caenorhabditis elegans*. Curr Biol. 2001; 11(24):1975–80. https://doi.org/10.1016/s0960-9822(01)00594-2 PMID: 11747825

29. Lin K, Hsin H, Libina N, Kenyon C. Regulation of the *Caenorhabditis elegans* longevity protein DAF-16 by insulin/IGF-1 and germline signaling. Nat Genet. 2001; 28(2):139–45. https://doi.org/10.1038/88850 PMID: 11381260

30. Kwon ES, Narasimhan SD, Yen K, Tissenbaum HA. A new DAF-16 isoform regulates longevity. Nature. 2010; 466(7305):498–502. https://doi.org/10.1038/nature09184 PMID: 20613724

31. Tepper RG, Ashraf J, Kaletsky R, Kleemann G, Murphy CT, Bussemaker HJ. PQM-1 complements DAF-16 as a key transcriptional regulator of DAF-2-mediated development and longevity. Cell. 2013; 154(3):676–90. https://doi.org/10.1016/j.cell.2013.07.006 PMID: 23911329

32. Zhang Y-P, Zhang W-H, Zhang P, Li Q, Sun Y, Wang J-W, et al. Degrading intestinal DAF-2 nearly doubles *Caenorhabditis elegans* lifespan without affecting development or reproduction. bioRxiv. 2021. https://doi.org/10.1101/2021.07.31.454567

33. Aghayeva U, Bhattacharya A, Hobert O. A panel of fluorophore-tagged daf-16 alleles. MicroPubl Biol. 2020; 2020. https://doi.org/10.17912/micropub.biology.000210 PMID: 32550509

34. Bhattacharya A, Aghayeva U, Berghoff EG, Hobert O. Plasticity of the Electrical Connectome of *C. elegans*. Cell. 2019; 176(5):1174–89 e16. https://doi.org/10.1016/j.cell.2018.12.024 PMID: 30686580

35. Clokey GV, Jacobson LA. The autofluorescent "lipofuscin granules" in the intestinal cells of Caenorhabditis elegans are secondary lysosomes. Mech Ageing Dev. 1986; 35(1):79–94. https://doi.org/10.1016/0047-6374(86)90068-0 PMID: 3736133

36. Hermann GJ, Schroeder LK, Hieb CA, Kershner AM, Rabbitts BM, Fonarev P, et al. Genetic analysis of lysosomal trafficking in *Caenorhabditis elegans*. Mol Biol Cell. 2005; 16(7):3273–88. https://doi.org/10.1091/mbc.e05-01-0060 PMID: 15843430

37. Coburn C, Allman E, Mahanti P, Benedetto A, Cabreiro F, Pincus Z, et al. Anthranilate fluorescence marks a calcium-propagated necrotic wave that promotes organismal death in *C. elegans*. PLoS Biol. 2013; 11(7):e1001613. https://doi.org/10.1371/journal.pbio.1001613 PMID: 23935448

38. Chavrier P, Parton RG, Hauri HP, Simons K, Zerial M. Localization of low molecular weight GTP binding proteins to exocytic and endocytic compartments. Cell. 1990; 62(2):317–29. https://doi.org/10.1016/0092-8674(90)90369-p PMID: 2115402

39. Sato M, Sato K, Fonarev P, Huang CJ, Liou W, Grant BD. *Caenorhabditis elegans* RME-6 is a novel regulator of RAB-5 at the clathrin-coated pit. Nat Cell Biol. 2005; 7(6):559–69. https://doi.org/10.1038/ncb1261 PMID: 15895077

40. Chen CC, Schweinsberg PJ, Vashist S, Mareiniss DP, Lambie EJ, Grant BD. RAB-10 Is Required for Endocytic Recycling in the *Caenorhabditis elegans* Intestine. Mol Biol Cell. 2006; 17(3):1286–97. https://doi.org/10.1091/mbc.e05-08-0787 PMID: 16394106

41. Swanson MM, Riddle DL. Critical periods in the development of the *Caenorhabditis elegans* dauer larva. Dev Biol. 1981; 84(1):27–40. https://doi.org/10.1016/0012-1606(81)90367-5 PMID: 7250500

42. Ogg S, Ruvkun G. The C. elegans PTEN homolog, DAF-18, acts in the insulin receptor-like metabolic signaling pathway. Mol Cell. 1998; 2(6):887–93. https://doi.org/10.1016/s1097-2765(00)80303-2 PMID: 9885576

43. Paradis S, Ruvkun G. *Caenorhabditis elegans* Akt/PKB transduces insulin receptor-like signals from AGE-1 PI3 kinase to the DAF-16 transcription factor. Genes Dev. 1998; 12(16):2488–98. https://doi.org/10.1101/gad.12.16.2488 PMID: 9716402

44. Hertweck M, Gobel C, Baumeister R. *C. elegans* SGK-1 is the critical component in the Akt/PKB kinase complex to control stress response and life span. Dev Cell. 2004; 6(4):577–88. https://doi.org/10.1016/s1534-5807(04)00095-4 PMID: 15068796

45. Jones KT, Greer ER, Pearce D, Ashrafi K. Rictor/TORC2 regulates *Caenorhabditis elegans* fat storage, body size, and development through *sgk-1*. PLoS Biol. 2009; 7(3):e60. https://doi.org/10.1371/journal.pbio.1000060 PMID: 19260765

46. Brunet A, Bonni A, Zigmond MJ, Lin MZ, Juo P, Hu LS, et al. Akt promotes cell survival by phosphorylating and inhibiting a Forkhead transcription factor. Cell. 1999; 96(6):857–68. https://doi.org/10.1016/s0092-8674(00)80595-4 PMID: 10102273

47. Wang Y, Oh SW, Deplancke B, Luo J, Walhout AJ, Tissenbaum HA. *C. elegans* 14-3-3 proteins regulate life span and interact with SIR-2.1 and DAF-16/FOXO. Mech Ageing Dev. 2006; 127(9):741–7. https://doi.org/10.1016/j.mad.2006.05.005 PMID: 16860373

48. Morton DG, Shakes DC, Nugent S, Dichoso D, Wang W, Golden A, et al. The *Caenorhabditis elegans par-5* gene encodes a 14-3-3 protein required for cellular asymmetry in the early embryo. Dev Biol. 2002; 241(1):47–58. https://doi.org/10.1006/dbio.2001.0489 PMID: 11784094

49. Wang W, Shakes DC. Expression patterns and transcript processing of *ftt-1* and *ftt-2*, two *C. elegans* 14-3-3 homologues. J Mol Biol. 1997; 268(3):619–30. https://doi.org/10.1006/jmbi.1997.1002 PMID: 9171285

50. Kimura KD, Tissenbaum HA, Liu Y, Ruvkun G. *daf-2*, an insulin receptor-like gene that regulates longevity and diapause in *Caenorhabditis elegans*. Science. 1997; 277(5328):942–6. https://doi.org/10.1126/science.277.5328.942 PMID: 9252323

51. O'Rourke EJ, Soukas AA, Carr CE, Ruvkun G. *C. elegans* major fats are stored in vesicles distinct from lysosome-related organelles. Cell Metab. 2009; 10(5):430–5. https://doi.org/10.1016/j.cmet.2009.10.002 PMID: 19883620

52. Escorcia W, Ruter DL, Nhan J, Curran SP. Quantification of Lipid Abundance and Evaluation of Lipid Distribution in Caenorhabditis elegans by Nile Red and Oil Red O Staining. J Vis Exp. 2018;(133). https://doi.org/10.3791/57352 PMID: 29553519

53. Honda Y, Honda S. The *daf-2* gene network for longevity regulates oxidative stress resistance and Mn-superoxide dismutase gene expression in *Caenorhabditis elegans*. FASEB journal 1999; 13(11):1385–93. PMID: 10428762

54. Murphy CT, McCarroll SA, Bargmann CI, Fraser A, Kamath RS, Ahringer J, et al. Genes that act downstream of DAF-16 to influence the lifespan of *Caenorhabditis elegans*. Nature. 2003; 424(6946):277–83. https://doi.org/10.1038/nature01789 PMID: 12845331

55. Ackerman D, Gems D. Insulin/IGF-1 and hypoxia signaling act in concert to regulate iron homeostasis in Caenorhabditis elegans. PLoS Genet. 2012; 8(3):e1002498. https://doi.org/10.1371/journal.pgen.1002498 PMID: 22396654

56. Miaczynska M. Effects of membrane trafficking on signaling by receptor tyrosine kinases. Cold Spring Harbor perspectives in biology. 2013; 5(11):a009035. https://doi.org/10.1101/cshperspect.a009035 PMID: 24186066

57. Kim Y, Shiba-Ishii A, Nakagawa T, Iemura SI, Natsume T, Nakano N, et al. Stratifin regulates stabilization of receptor tyrosine kinases via interaction with ubiquitin-specific protease 8 in lung adenocarcinoma. Oncogene. 2018; 37(40):5387–402. https://doi.org/10.1038/s41388-018-0342-9 PMID: 29880877

58. Khan MN, Savoie S, Bergeron JJ, Posner BI. Characterization of rat liver endosomal fractions. In vivo activation of insulin-stimulable receptor kinase in these structures. J Biol Chem. 1986; 261(18):8462–72. PMID: 3522569

59. Balbis A, Baquiran G, Bergeron JJ, Posner BI. Compartmentalization and insulin-induced translocations of insulin receptor substrates, phosphatidylinositol 3-kinase, and protein kinase B in rat liver. Endocrinology. 2000; 141(11):4041–9. https://doi.org/10.1210/endo.141.11.7774 PMID: 11089534

60. Christoforidis S, Miaczynska M, Ashman K, Wilm M, Zhao L, Yip SC, et al. Phosphatidylinositol-3-OH kinases are Rab5 effectors. Nat Cell Biol. 1999; 1(4):249–52. https://doi.org/10.1038/12075 PMID: 10559924

61. Braccini L, Ciraolo E, Campa CC, Perino A, Longo DL, Tibolla G, et al. PI3K-C2gamma is a Rab5 effector selectively controlling endosomal Akt2 activation downstream of insulin signalling. Nature communications. 2015; 6:7400. https://doi.org/10.1038/ncomms8400 PMID: 26100075

62. Mondin VE, Ben El Kadhi K, Cauvin C, Jackson-Crawford A, Belanger E, Decelle B, et al. PTEN reduces endosomal PtdIns(4,5)P2 in a phosphatase-independent manner via a PLC pathway. J Cell Biol. 2019; 218(7):2198–214. https://doi.org/10.1083/jcb.201805155 PMID: 31118240

63. Shinde SR, Maddika S. PTEN Regulates Glucose Transporter Recycling by Impairing SNX27 Retromer Assembly. Cell Rep. 2017; 21(6):1655–66. https://doi.org/10.1016/j.celrep.2017.10.053 PMID: 29117568

64. Hsu JW, Bai M, Li K, Yang JS, Chu N, Cole PA, et al. The protein kinase Akt acts as a coat adaptor in endocytic recycling. Nat Cell Biol. 2020; 22(8):927–33. https://doi.org/10.1038/s41556-020-0530-z PMID: 32541877

65. Shin HW, Hayashi M, Christoforidis S, Lacas-Gervais S, Hoepfner S, Wenk MR, et al. An enzymatic cascade of Rab5 effectors regulates phosphoinositide turnover in the endocytic pathway. J Cell Biol. 2005; 170(4):607–18. https://doi.org/10.1083/jcb.200505128 PMID: 16103228

66. Su X, Lodhi IJ, Saltiel AR, Stahl PD. Insulin-stimulated Interaction between insulin receptor substrate 1 and p85alpha and activation of protein kinase B/Akt require Rab5. J Biol Chem. 2006; 281(38):27982–90. https://doi.org/10.1074/jbc.M602873200 PMID: 16880210

67. Cheng KK, Iglesias MA, Lam KS, Wang Y, Sweeney G, Zhu W, et al. APPL1 potentiates insulin-mediated inhibition of hepatic glucose production and alleviates diabetes via Akt activation in mice. Cell Metab. 2009; 9(5):417–27. https://doi.org/10.1016/j.cmet.2009.03.013 PMID: 19416712

68. Zeigerer A, Bogorad RL, Sharma K, Gilleron J, Seifert S, Sales S, et al. Regulation of liver metabolism by the endosomal GTPase Rab5. Cell Rep. 2015; 11(6):884–92. https://doi.org/10.1016/j.celrep.2015.04.018 PMID: 25937276

69. Kang C, Xu Q, Martin TD, Li MZ, Demaria M, Aron L, et al. The DNA damage response induces inflammation and senescence by inhibiting autophagy of GATA4. Science. 2015; 349(6255):aaa5612. https://doi.org/10.1126/science.aaa5612 PMID: 26404840

70. Berman JR, Kenyon C. Germ-cell loss extends *C. elegans* life span through regulation of DAF-16 by *kri-1* and lipophilic-hormone signaling. Cell. 2006; 124(5):1055–68. https://doi.org/10.1016/j.cell.2006.01.039 PMID: 16530050

71. Moll L, Roitenberg N, Bejerano-Sagie M, Boocholez H, Carvalhal Marques F, Volovik Y, et al. The insulin/IGF signaling cascade modulates SUMOylation to regulate aging and proteostasis in *Caenorhabditis elegans*. Elife. 2018; 7. https://doi.org/10.7554/eLife.38635 PMID: 30403374

72. Kershner AM, Shin H, Hansen TJ, Kimble J. Discovery of two GLP-1/Notch target genes that account for the role of GLP-1/Notch signaling in stem cell maintenance. Proc Natl Acad Sci U S A. 2014; 111(10):3739–44. https://doi.org/10.1073/pnas.1401861111 PMID: 24567412

73. Robida-Stubbs S, Glover-Cutter K, Lamming DW, Mizunuma M, Narasimhan SD, Neumann-Haefelin E, et al. TOR signaling and rapamycin influence longevity by regulating SKN-1/Nrf and DAF-16/FoxO. Cell Metab. 2012; 15(5):713–24. https://doi.org/10.1016/j.cmet.2012.04.007 PMID: 22560223

74. Oh SW, Mukhopadhyay A, Svrzikapa N, Jiang F, Davis RJ, Tissenbaum HA. JNK regulates lifespan in *Caenorhabditis elegans* by modulating nuclear translocation of forkhead transcription factor/DAF-16. Proc Natl Acad Sci U S A. 2005; 102(12):4494–9. https://doi.org/10.1073/pnas.0500749102 PMID: 15767565

75. Greer EL, Dowlatshahi D, Banko MR, Villen J, Hoang K, Blanchard D, et al. An AMPK-FOXO pathway mediates longevity induced by a novel method of dietary restriction in *C. elegans*. Curr Biol. 2007; 17(19):1646–56. https://doi.org/10.1016/j.cub.2007.08.047 PMID: 17900900

76. Sancak Y, Peterson TR, Shaul YD, Lindquist RA, Thoreen CC, Bar-Peled L, et al. The Rag GTPases bind raptor and mediate amino acid signaling to mTORC1. Science. 2008; 320(5882):1496–501. https://doi.org/10.1126/science.1157535 PMID: 18497260

77. Sun X, Chen WD, Wang YD. DAF-16/FOXO Transcription Factor in Aging and Longevity. Front Pharmacol. 2017; 8:548. https://doi.org/10.3389/fphar.2017.00548 PMID: 28878670

78. Melendez A, Talloczy Z, Seaman M, Eskelinen EL, Hall DH, Levine B. Autophagy genes are essential for dauer development and life-span extension in *C. elegans*. Science. 2003; 301(5638):1387–91. https://doi.org/10.1126/science.1087782 PMID: 12958363

79. Ruck A, Attonito J, Garces KT, Nunez L, Palmisano NJ, Rubel Z, et al. The Atg6/Vps30/Beclin 1 ortholog BEC-1 mediates endocytic retrograde transport in addition to autophagy in *C. elegans*. Autophagy. 2011; 7(4):386–400. https://doi.org/10.4161/auto.7.4.14391 PMID: 21183797

80. Law F, Seo JH, Wang Z, DeLeon JL, Bolis Y, Brown A, et al. The VPS34 PI3K negatively regulates RAB-5 during endosome maturation. J Cell Sci. 2017; 130(12):2007–17. https://doi.org/10.1242/jcs.194746 PMID: 28455411

81. Hars ES, Qi H, Ryazanov AG, Jin S, Cai L, Hu C, et al. Autophagy regulates ageing in *C. elegans*. Autophagy. 2007; 3(2):93–5. https://doi.org/10.4161/auto.3636 PMID: 17204841

82. Samuelson AV, Carr CE, Ruvkun G. Gene activities that mediate increased life span of *C. elegans* insulin-like signaling mutants. Genes Dev. 2007; 21(22):2976–94. https://doi.org/10.1101/gad.1588907 PMID: 18006689

83. Lapierre LR, De Magalhaes Filho CD, McQuary PR, Chu CC, Visvikis O, Chang JT, et al. The TFEB orthologue HLH-30 regulates autophagy and modulates longevity in *Caenorhabditis elegans*. Nature communications. 2013; 4:2267. https://doi.org/10.1038/ncomms3267 PMID: 23925298

84. Guo B, Huang X, Zhang P, Qi L, Liang Q, Zhang X, et al. Genome-wide screen identifies signaling pathways that regulate autophagy during *Caenorhabditis elegans* development. EMBO Rep. 2014; 15(6):705–13. https://doi.org/10.1002/embr.201338310 PMID: 24764321

85. Sun Y, Li M, Zhao D, Li X, Yang C, Wang X. Lysosome activity is modulated by multiple longevity pathways and is important for lifespan extension in C. *elegans*. Elife. 2020; 9. https://doi.org/10.7554/eLife.55745 PMID: 32482227

86. Behrends C, Sowa ME, Gygi SP, Harper JW. Network organization of the human autophagy system. Nature. 2010; 466(7302):68–76. https://doi.org/10.1038/nature09204 PMID: 20562859

87. Popovic D, Akutsu M, Novak I, Harper JW, Behrends C, Dikic I. Rab GTPase-activating proteins in autophagy: regulation of endocytic and autophagy pathways by direct binding to human ATG8 modifiers. Mol Cell Biol. 2012; 32(9):1733–44. https://doi.org/10.1128/MCB.06717-11 PMID: 22354992

88. Carroll B, Mohd-Naim N, Maximiano F, Frasa MA, McCormack J, Finelli M, et al. The TBC/RabGAP Armus coordinates Rac1 and Rab7 functions during autophagy. Dev Cell. 2013; 25(1):15–28. https://doi.org/10.1016/j.devcel.2013.03.005 PMID: 23562278

89. Toyofuku T, Morimoto K, Sasawatari S, Kumanogoh A. Leucine-Rich Repeat Kinase 1 Regulates Autophagy through Turning On TBC1D2-Dependent Rab7 Inactivation. Mol Cell Biol. 2015; 35 (17):3044–58. https://doi.org/10.1128/MCB.00085-15 PMID: 26100023

90. Kamath RS, Martinez-Campos M, Zipperlen P, Fraser AG, Ahringer J. Effectiveness of specific RNA-mediated interference through ingested double-stranded RNA in *Caenorhabditis elegans*. Genome Biol. 2001; 2(1):RESEARCH0002. https://doi.org/10.1186/gb-2000-2-1-research0002 PMID: 11178279

91. Fraser AG, Kamath RS, Zipperlen P, Martinez-Campos M, Sohrmann M, Ahringer J. Functional genomic analysis of *C. elegans* chromosome I by systematic RNA interference. Nature. 2000; 408 (6810):325–30. https://doi.org/10.1038/35042517 PMID: 11099033

92. Kamath RS, Fraser AG, Dong Y, Poulin G, Durbin R, Gotta M, et al. Systematic functional analysis of the *Caenorhabditis elegans* genome using RNAi. Nature. 2003; 421(6920):231–7. https://doi.org/10.1038/nature01278 PMID: 12529635

93. Timmons L, Fire A. Specific interference by ingested dsRNA. Nature. 1998; 395(6705):854. https://doi.org/10.1038/27579 PMID: 9804418

94. Gems D, Riddle DL. Defining wild-type life span in *Caenorhabditis elegans*. J Gerontol A Biol Sci Med Sci. 2000; 55(5):B215–9. https://doi.org/10.1093/gerona/55.5.b215 PMID: 10819307

95. Zhao Y, Wang H, Poole RJ, Gems D. A *fln-2* mutation affects lethal pathology and lifespan in *C. elegans*. Nature communications. 2019; 10(1):5087. https://doi.org/10.1038/s41467-019-13062-z PMID: 31704915

96. Ratemi Z, Kiss R, Rocheleau C. *C. elegans rab-18* mutants display reduced lipid content under fed and fasted conditions. MicroPubl Biol. 2019; 2019. https://doi.org/10.17912/micropub.biology.000188 PMID: 32550463

97. Senchuk MM, Dues DJ, Schaar CE, Johnson BK, Madaj ZB, Bowman MJ, et al. Activation of DAF-16/FOXO by reactive oxygen species contributes to longevity in long-lived mitochondrial mutants in *Caenorhabditis elegans*. PLoS Genet. 2018; 14(3):e1007268. https://doi.org/10.1371/journal.pgen.1007268 PMID: 29522556